

Generalized Fibonacci Matrices in Medicine

A.G. Shannon

Warrane College, University of New South Wales,
PO Box 123, Kensington, NSW 1465, Australia
t.shannon@warrane.unsw.edu.au

Abstract

Medical measurements, by their very nature, are array-oriented. Matrices are, in a sense, their natural medium of display. Fibonacci matrices, given the natural growth modeling of second order linear sequences, are then particularly suitable vehicles for displaying, developing and discussing medical phenomena. This paper illustrates some of these aspects, partly for their pure mathematical elegance, and partly for their applied mathematical aptness.

Keywords: Fibonacci numbers, recurrence relations, false positives, diabetes mellitus, breast cancer, mammography, ultrasonography.

AMS Classifications: 92B05, 11B39, 11C20.

1. Introduction

Medical data are often reported at discrete time intervals as in Table 1, in which the measurements are for thirteen different patients with non-insulin dependent diabetes mellitus. It makes sense then to use discrete mathematics in medical modeling rather than to interpolate between the measurements in order to utilize traditional analytic methods. The array in Table 1 is a matrix, and matrices have many simple mathematical properties which can both illuminate the processes and speed up the calculations. It is the purpose of this paper to illustrate these ideas with some examples.

1	2	3	4	5	6	7	8	9	10	11	12	13	14
-30	205	390	210	270	130	465	160	170	180	125	115	150	115
0	200	390	220	270	125	470	160	165	180	120	115	145	115
10	145	380	155	270	120	465	140	150	160	110	95	95	105
20	105	355	90	245	90	450	110	100	135	75	55	70	85
30	75	345	70	220	70	445	100	85	130	20	45	40	65
40	60	325	65	200	70	430	90	75	120	30	40	25	60
50	40	330	55	190	70	410	80	60	120	30	40	40	55
60	60	325	50	185	65	400	70	55	115	30	35	45	55
70	80	310	60	180	60	390	70	55	105	35	30	45	55
80	100	310	80	180	55	380	70	60	105	40	30	45	60
90	110	310	95	180	60	385	80	65	105	55	55	50	65

Table 1: Plasma Glucose (mg/100ml) (Columns 2-14) versus Time (minutes) (Column 1)

2. Fibonacci Growth

Heyde [6] pointed out the advantages of a model which incorporates “an immature phase during which individuals do not reproduce. Such behaviour is common in nature and cannot be satisfactorily modeled by the ordinary Bienaymé-Galton-Watson process”. Makhmudov [13] applied this to the process of spreading infectious diseases with three stages: (i) an initial stage of k periods, during which those who are ill with the disease do not infect others; a mature stage of l periods when each person affects $n(t)$ of healthy people; and (iii) a recovery stage when each individual recovers r periods after initial infection. For instance, in the case of the common cold we often get (on average) $k = 2, l = 3, r = 7$ [16]. Since APL is an array-oriented programming language with the advantage of both arithmetical and logical operations between matrices, code for Makhmudov’s model is listed in Table 1, with the output when $k = 2, l = r = 15$, displayed in Table 2 since that yields the Fibonacci sequence in the final column. (Note that the other eight columns display $C(n, j)$ for $j = 0, 1, 2, \dots, 7$.) For other pertinent generalizations, see [14].

```

      ▽DISEASE1[0]▽
      ▽1 DISEASE1 K
[1]  “COEFFICIENTS FOR GENERAL TERM IN SPREAD OF DISEASE:
[2]  “LEFT ARGUMENT-NUMBERS OF ROWS AND COLUMNS IN ARRAY:
[3]  “RIGHT ARGUMENT-K,L AND R.
[4]  A←!p0 ∘ R←C←1
[5]  L1:A[R:C]←1
[6]  →((! [1]≥R) ∧ (K[3]≥R←R+1))/L1
[7]  L2:C+C+1∠R←((C-1)×K[1])+1
[8]  →((( [1]<R←R+1) ∧ (C=A[R:C]←C))∨((! [1]<R←R+1) ∧ (A[R:C]←1))∨((! [2]≤C)∨(! [1]≤R)))/END
[9]  L3:D←0
[10] L4:A[R:C]←A[(R-D+K[1]);(C-10)+A[R:C]
[11] →((0<R-D+K[1]) ∧ (K[2]>D←D+1))/L4
[12] →(! [1]≥R←R+1)/L3
[13] →L2
[14] END:A,+A
      ▽

```

Table 2: An APL program for Makhmudov’s model

	14	8	DISEASE1	2	15	15		
1	0	0	0	0	0	0	0	1
1	0	0	0	0	0	0	0	1
1	1	0	0	0	0	0	0	2
1	2	0	0	0	0	0	0	3
1	3	1	0	0	0	0	0	5
1	4	3	0	0	0	0	0	8
1	5	6	1	0	0	0	0	13
1	6	10	4	0	0	0	0	21
1	7	15	10	1	0	0	0	34
1	8	21	20	5	0	0	0	55
1	9	28	35	15	1	0	0	89
1	10	36	56	35	6	0	0	144
1	11	45	84	70	21	1	0	233
1	12	55	120	126	56	7	0	377

Table 3: Application of the APL code

We notice incidentally that the columns, $j, j = 0, 1, 2, \dots, 8$, in Table 3 yield the sequences $\{C(n, j)\}$ for $j < 8$. For example, $\{C(n, 2)\}$ are the triangular numbers, $\{C(n, 3)\}$ are the tetrahedral numbers, while $\{C(n, 8)\}$ are obviously the Fibonacci numbers.

3. The Leslie Matrix

The elegance of properties is important in modeling, and a brief consideration of the Leslie matrix [11] illustrates this. Fibonacci growth arises quite naturally in matrix representation. As an illustration we express the dynamics of Fibonacci growth in Leslie matrix form and relate this to other known matrices and second order sequences.

$$L_{n \times n} = \begin{bmatrix} 0 & 1 & 1 & \dots & 1 & 1 \\ 1 & 0 & 0 & \dots & 0 & 0 \\ 0 & 1 & 0 & \dots & 0 & 0 \\ & & & \dots & & \\ 0 & 0 & 0 & \dots & 0 & 0 \\ 0 & 0 & 0 & \dots & 1 & 1 \end{bmatrix} \quad (3.1)$$

First row elements represent births of two offspring to each mating pair in generation t , and subdiagonal elements represent survival of each year class (here 100%). The final diagonal element confers immortality to the population. When this element is zero, L becomes the more familiar Q matrix. The Leslie matrix is also related to generalizations of the continued fraction algorithm [15].

If we consider

$$L'_{n \times n} = [l'_{i,j}{}^{(r)}],$$

then it can be readily established that for $n > 2$,

$$\sum_{i=1}^n l'_{i,j}{}^{(r)} = \begin{cases} F_{r+1}, & j = 1, \\ F_{r+2}, & j > 1, \end{cases} \quad (3.2)$$

and

$$\sum_{j=1}^n l'_{i,j}{}^{(r)} = \begin{cases} U_{r+1,r+1}, & i = 1, \\ U_{r+1,r}, & i = 2, \end{cases} \quad (3.3)$$

in which $\{U_{r,m}\}$ is an integer sequence which satisfies the second order generalized Fibonacci linear homogeneous recurrence relation (1.1) in the form

$$U_{r,m} = U_{r,m-1} + U_{r,m-2}, \quad m > 2, \quad (3.4)$$

with initial conditions $U_{r,1} = 1, U_{r,2} = n - 1$. When $n = 2$, we get the ordinary Fibonacci sequence $\{F_n\}$. The first few examples of this sequence are displayed in Table 4.

$m =$	1	2	3	4	5	6	7
$\{U_{3,m}\}$	1	2	3	5	8	13	21
$\{U_{4,m}\}$	1	3	4	7	11	18	29
$\{U_{5,m}\}$	1	4	5	9	14	23	37
$\{U_{6,m}\}$	1	5	6	11	17	28	45

Table 4: $\{U_{r,m}\}$, $r=3,4,5,6$; $m=1,2,\dots,7$

As a further illustration, we can see that for $r = 4$, and $n = 5$,

$$\begin{bmatrix} 0 & 1 & 1 & 1 & 0 \\ 1 & 0 & 0 & 0 & 0 \\ 0 & 1 & 0 & 0 & 0 \\ 0 & 0 & 1 & 0 & 0 \\ 0 & 0 & 0 & 1 & 1 \end{bmatrix}^4 = \begin{bmatrix} 2 & 3 & 3 & 3 & 3 \\ 1 & 2 & 2 & 2 & 2 \\ 1 & 1 & 1 & 1 & 1 \\ 0 & 1 & 1 & 1 & 1 \\ 1 & 1 & 1 & 1 & 1 \end{bmatrix}$$

so that, in turn,

$$\begin{aligned} \sum_{i=1}^5 l_{i,1}^{(4)} &= 5 = F_5, \\ \sum_{i=1}^5 l_{i,2}^{(4)} &= 8 = F_6, \\ \sum_{j=1}^5 l_{1,j}^{(4)} &= 14 = U_{5,5}, \\ \sum_{j=1}^5 l_{2,j}^{(4)} &= 9 = U_{5,4}. \end{aligned}$$

Note further, that if we treat (3.4) as a partial difference equation, then

$$U_{r+1,m} - U_{r,m-1} = F_{m-1}, m > 2, \quad (3.5)$$

and, furthermore,

$$\begin{aligned} \{U_{3,m}\} &= \{F_{m+1}\}, \\ \{U_{4,m}\} &= \{L_m\}, \\ \{U_{5,m}\} &= \{T_m\}, \end{aligned}$$

$\{L_m\}$ is the well-known sequence of Lucas numbers, and $\{T_m\}$ is a sequence first investigated by Brousseau [1].

4. A Diabetes Example

The purpose of this research was to compare the rates of absorption of insulin administered intravenously (IV) and subcutaneously (SC) in humans. Experiments with rats suggest that significant inactivation of the insulin occurs at or near the injection site when it is administered subcutaneously in the usual way [18].

Insulin promotes lipid synthesis and inhibits lipid breakdown which causes an increase in body weight with excess dosage. Hyperinsulinaemia causes a breakdown in the regulations of the insulin receptor. This exaggerates the insulin resistant state already in existence in over-insulined T1D patients or in T2D obese patients. We effectively have a two-compartment model (Figure 1) in which x_i is the concentration of insulin in Compartment i at time t_i . It is assumed that insulin can flow from SC into IV, but not from IV into SC, and that the clearance rates k from each compartment are constant:

- k_a represents a subcutaneous injection,
- k_{12} represents the flow of insulin from the SC tissue to the veins, and
- k_c, k_d represents the disappearance (metabolic or otherwise) of the insulin [2].

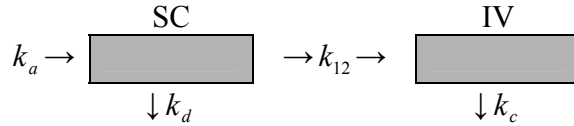


Figure 1

The problem is to consider a steady infusion rate $k(t)$ appropriate units of insulin per minute into the IV compartment. This can be represented by a one-compartment model (Figure 2) since there is no feedback from IV to SC.



Figure 2

The differential equation which represents the amount of insulin administered IV, x , at time t is then

$$\frac{dx}{dt} = -k_c x + i(t), \quad x(0) = 0, \quad (4.1)$$

We used a commonly accepted clearance rate of $k_c = 10\%$ of volume per minute, though individual clearance rates can be found by curve-fitting techniques [3]. Our problem now is to find the insulin infusion rate $i(t)$ which makes the IV profile given by Equation (4.1) fit as closely as possible to the subcutaneous profile $s(t)$ over a given period of T minutes. Equation (4.1) can be solved by the Laplace convolution theorem and then discretized to yield

$$\begin{aligned} x_n &= x(n\Delta t) = x(t) \\ &= \exp(-k_c t) \sum_{r=1}^n I_r \int_{(r-1)\Delta t}^{r\Delta t} \exp(k_c \tau) d\tau. \end{aligned} \quad (4.2)$$

Setting

$$a_{nr} = \frac{1}{k_c} (1 - \exp(-k_c \Delta t)) \exp(-k_c (n-r)\Delta t) \quad (4.3)$$

we get the recurrence relation

$$a_{n+1,r} = \exp(-k_c \Delta t) a_{nr} \quad (4.4)$$

and

$$x_n = \sum_{r=1}^n a_{nr} I_r. \quad (4.5)$$

Our least squares problem is now to find the set of intravenous injection rates I_r , $r = 1, 2, \dots, N$, so as to minimize

$$D = \sum_{n=1}^N (x_n - s_n)^2 \quad (4.6)$$

in which s_n is the value of the SC profile at time $n\Delta t (= t)$, $N\Delta t = T$. Let

$$\alpha_{nk} = \begin{cases} 0 & n < k, \\ 1 & n \geq k, \end{cases}$$

and

$$A = [a_{kj} \alpha_{kj}],$$

a triangular matrix. Then,

$$A^T A \dot{i} = A^T \underline{s} \quad (4.7)$$

where

$$\underline{s} = [s_1, s_2, \dots, s_N]^T, \\ \dot{i} = [I_1, I_2, \dots, I_N]^T.$$

For example, when $N = 3$,

$$\begin{bmatrix} a_{11} & a_{21} & a_{31} \\ 0 & a_{22} & a_{32} \\ 0 & 0 & a_{33} \end{bmatrix} \begin{bmatrix} a_{11} & 0 & 0 \\ a_{21} & a_{22} & 0 \\ a_{31} & a_{32} & a_{33} \end{bmatrix} \begin{bmatrix} I_1 \\ I_2 \\ I_3 \end{bmatrix} = \begin{bmatrix} a_{11} & a_{21} & a_{31} \\ 0 & a_{22} & a_{32} \\ 0 & 0 & a_{33} \end{bmatrix} \begin{bmatrix} s_1 \\ s_2 \\ s_3 \end{bmatrix}.$$

From (4.7) we obtain

$$\dot{i} = A^{-1} \underline{s} \quad (4.7)$$

which is the set of intravenous infusion rates. $A^T A$ is a Cholesky decomposition which is utilized in the next section with a generalized Fibonacci recurrence relation [7]. (Well-documented error analyses exist for Cholesky decompositions [21])

5. A Breast Cancer Example

Mammography is a means of detecting breast cancer before a mass can be felt by a physical breast examination. However, because of the non-specificity of the mammographic appearance of many malignant lesions, false positives can occur [5]. Ultrasonography is therefore used as a complement to mammography because the ultrasound characteristics of malignant lesions are often highlighted in dense parenchyma (the functional elements of an organ) and cystic lesions can usually be differentiated from solid masses [4].

Breast tissue is glandular, fibrous, and fatty, the last of which is the main bulk of the breast. Let

- U be the ultrasound energy transmitted,
- M be the metabolic energy generated,
- P be the thermal energy carried away by perfusion, and
- S be the thermal energy lost by emission from the skin.

Figure 3 shows the energy distribution of these variables when ultrasound is directed onto the skin in the direction of the suspected lesion.

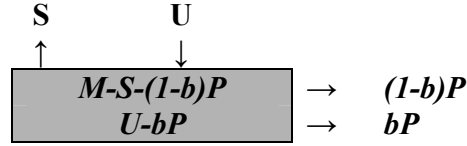


Figure 3: Ultrasound energy transfer

Diagnostic sound waves can only be transmitted in solids and liquids because they utilize a frequency range between 1 and 10 million hertz (1×10^6 cycles per second). By way of comparison, a frequency range of 20 to 20,000 cycles per second provides stimulation of the subjective sensation of hearing [20]. When an ultrasound beam passes through tissue, energy is partly absorbed and converted to heat. This causes a rise in tissue temperature which depends on several factors such as the heat conduction and transport by blood flow from the exposed tissue into surrounding regions. Figure 4 is a flow diagram to link these energy components.

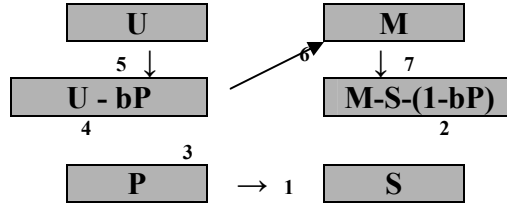


Figure 4: The flow diagram

If bP represents that part of the ultrasound energy which is absorbed and carried away by perfusion ($0 \leq b \leq 1$), then $U-bP$ is the ultrasound energy which reaches the lesion. (Perfusion in general is forcing fluid through an organ by way of blood vessels.) Since it is generally recognized that there is increased metabolic activity within breast tumours, we can assume that the ultrasound energy received on the lesion will increase the local metabolic activity as formulated in

$$M(t) - M(t-1) = \mu[CU(t-1) - bP(t-1)] \quad (5.1)$$

The metabolic energy that remains after deducting part of it due to the energy lost from the skin and perfusion is $M-S-(1-b)P$. Since increased blood flow is associated with increased metabolic activity [12], the increase in perfusion rate is associated with the increase in this remaining metabolic energy as expressed in

$$P(t) - P(t-1) = \lambda[M(t-1) - S(t-1) - (1-b)P(t-1)] \quad (5.2)$$

Furthermore, skin temperature results primarily from blood perfusion to the tissues and the blood flow in the superficial veins [12], as represented by

$$S(t) = aP(t). \quad (5.3)$$

The matrix form of Equations (5.1)-(5.3) is

$$\begin{bmatrix} 1 & -a & 0 \\ 0 & 1 & 0 \\ 0 & 0 & 1 \end{bmatrix} \begin{bmatrix} S(t) \\ P(t) \\ M(t) \end{bmatrix} = \begin{bmatrix} 0 & 0 & 0 \\ -\lambda & 1 - \lambda(1-b) & \lambda \\ 0 & -b\mu & 1 \end{bmatrix} + \begin{bmatrix} 0 \\ 0 \\ \mu U(t-1) \end{bmatrix}. \quad (5.4)$$

Since the ultrasound energy applied at the surface is constant, we set $k = U(t-2)$, and for notational convenience we express $S(t)/S(t_0)$ as S_t , so we can rewrite Equation (5.4) as the second order inhomogeneous recurrence relation [9]

$$S_t - [2 - \lambda a - \lambda(1-b)]S_{t-1} - [\lambda a - 1 + \lambda(1-b) - \lambda\mu b]S_{t-2} = a\lambda\mu k / S(t_0). \quad (5.5)$$

Horadam and Shannon [8] expounded a method for solving generalized inhomogeneous equations of this form which can be rewritten as

$$S_t = \sum_{j=1}^3 B_j S_{t-j}, \quad (5.6)$$

where S_{t-3} is treated as unity, $t = 0, 1, \dots, n$, with $n+1$ the number of experimental data points, and for notational convenience we let

$$\begin{aligned} B_1 &= 2 - \lambda a - \lambda(1-b), \\ B_2 &= \lambda a - 1 + \lambda(1-b) - \lambda\mu b, \\ B_3 &= a\lambda\mu k / S(t_0). \end{aligned}$$

The sum of squares of errors, SSE , has the form

$$SSE = \sum_{i=2}^n \left(S_i - \sum_{j=1}^3 B_j S_{i-j} \right)^2. \quad (5.7)$$

By differentiating (5.7) with respect to $B_i, i = 1, 2, 3$, and equating each of them to zero, three normal equations are obtained:

$$S\widehat{B} = E,$$

where

$$S = \begin{bmatrix} S_{11} & S_{12} & S_{13} \\ S_{21} & S_{22} & S_{23} \\ S_{31} & S_{32} & S_{33} \end{bmatrix}, E = \begin{bmatrix} E_1 \\ E_2 \\ E_3 \end{bmatrix}, \widehat{B} = \begin{bmatrix} \widehat{B}_1 \\ \widehat{B}_2 \\ \widehat{B}_3 \end{bmatrix},$$

the last being estimates, and where

$$\begin{aligned} S_{ij} &= \sum_{t=2}^n S_{t-i} S_{t-j} \\ E_i &= \sum_{t=2}^n S_t S_{t-i} \end{aligned}$$

Therefore,

$$\widehat{B} = S^{-1}E,$$

which can be solved by the Cholesky-Turing method since S is symmetric [10].

6. Concluding Comments

The parameters a, λ, μ were computed by fitting the model to thermal data. For example, the values in Table 5 are for several patients and where $b = 0.85$ which corresponds to a perfusion condition for a lesion approximately 5cm below the surface of the skin.

Patient	Remarks	D	a	λ	μ
A	Benign	1.9828	0.8050	1.6222	0.0757
B	Benign	2.3857	0.8144	2.2098	0.2869
C	Malignant	-1.4888	0.8491	2.7175	0.9589
D	Malignant	-1.2115	0.8409	1.8230	0.7220

Table 5: Results of fitting the model to experimental data

Where a malignant process is present, a differential cooling system occurs in the local skin surface prior to recovery to the initial skin temperature [19], where different responses (no recovery) were observed in benign lesions. It seems that if the response curve shows an initial cooling and $\mu > 0.7$, then a lesion may be present.

The generalized Fibonacci recurrence relation reasonably accounts for the thermal changes to the skin of the breast, and the associated matrix method presented here permits improved computational convenience.

References

1. Brousseau, Br Alfred. 1965. Seeking the Lost Gold Mine or Exploring for Fibonacci Factorization. *The Fibonacci Quarterly*. 3: 129-130.
2. Chiarella, C., A.G. Shannon. 1986. An Example of Diabetes Compartment Modelling. *Mathematical Modelling*. 7: 1239-1244.
3. Geraghty, D.P., A.G. Shannon, S. Colagiuri. 1986. Polynomial Curve-fitting of Clinical Data Arrays. *Journal of Clinical Computing*. 15(1): 29-32.
4. Harvey, J.A. 2007. Unusual Breast Cancers: Useful Clues to Expanding the Differential Diagnosis. *Radiology*. 242: 683-694.
5. Henderson, J.C. 1992. Breast Cancer Therapy – the Price of Success. *The New England Journal of Medicine*. 326: 1774-1775.
6. Heyde, C.C. 1981. On Fibonacci (or Lagged Bienaymé-Galton-Watson) Branching Processes. *Journal of Applied Probability*. 18:583-591.
7. Horadam, A.F., P. Filipponi. 1991. Cholesky Algorithm Matrices of Fibonacci Type and Properties of Generalized Sequences. *The Fibonacci Quarterly*. 19: 164-173.
8. Horadam, A.F., A.G. Shannon. 1988. Asveld's Polynomials $p_j(n)$. In A.N. Philippou, A.F. Horadam, G.E. Bergum (eds). *Applications of Fibonacci Numbers. Volume 2*. Dordrecht: Kluwer, pp.163-176.
9. Hung, W.T., A.G. Shannon, B.S. Thornton. 1994. The Use of a Second-order Recurrence Relation in the Diagnosis of Breast Cancer. *The Fibonacci Quarterly*. 32: 253-259.

10. Irving, J., N. Mullineux. 1964. *Mathematics in Physics and Engineering*. New York: Academic Press, pp.270-279.
11. Leslie, P.H. 1945. On the Use of Matrices in Certain Population Mathematics, *Biometrika*. 33 (1945): 183-212.
12. Love, T.J. 1980. Thermography as an Indicator of Blood Perfusion. *Annals of the New York Academy of Sciences*. 429-430.
13. Makhmudov, A. 1983. On Fibonacci's Model of Infectious Disease. In G.I. Marchuk, L.N. Belykh (eds). *Mathematical Modelling in Immunology and Medicine*. Amsterdam: North Holland, pp.319-323.
14. Moghaddamfar, A.R., S. Navid Salehy, S. Nima Salehy. 2008. Certain Matrices Related to the Fibonacci Sequence Having Recursive Entries. *Electronic Journal of Linear Algebra*. 17: 543-576.
15. Shannon, A.G., Leon Bernstein. 1973. The Jacobi-Perron Algorithm and the Algebra of Recursive Sequences. *Bulletin of the Australian Mathematical Society*. 8: 261-277.
16. Shannon, A.G. J.H. Clarke, L.J. Hills. 1987. Contingency Relations for Infectious Diseases. *Computing Mathematical Applications*. 14: 829-833.
17. Shannon, A.G., R.L. Ollerton, D.R. Owens. 1993. A Cholesky Decomposition in Matching Insulin Profiles. In G.E. Bergum, A.N. Philippou, A.F. Horadam (eds). *Applications of Fibonacci Numbers. Volume 5*. Dordrecht: Kluwer, pp.497-506.
18. Stevenson, R.W., T.I. Tsakok, J.A. Parsons. 1980. Matched Glucose Responses to Insulin Administered Subcutaneously and Intravenously. *Diabetologia*. 18: 423-426.
19. Thornton, B.S., W.T. Hung, C. Hirst. 1992. Diagnostic Model for Local Temporal Thermal Change at the Skin of the Breast during Extended Application of Diagnostic Ultrasound. *IMA Journal of Mathematics Applied in Medicine and Biology*. 9: 161-175.
20. Tortora, G.J., N.P. Anagnostakos. 1987. *Principles of Anatomy and Physiology, 5th Edition*. New York: Harper and Row, p.390.
21. Wilkinson, J.H. 1965. *The Algebraic Eigenvalue Problem*. Oxford: Clarendon Press.